All-optical quantum thermometry based on spin-level cross-relaxation and multicenter entanglement under ambient conditions in SiC

A. N. Anisimov,[1,a] V. A. Soltamov,[1,2] I. D. Breev,[1,3] R. A. Babunts,[1] E. N. Mokhov,[1] G. V. Astakhov,[1,2,4] V. Dyakonov,[2] D. R. Yakovlev,[1,5] D. Suter,[6] and P. G. Baranov[1,3]

[1]*Ioffe Institute, St Petersburg 194021, Russia*
[2]*Experimental Physics VI, Julius-Maximilian University of Würzburg, 97074 Würzburg, Germany*
[3]*Peter the Great St. Petersburg Polytechnic University, Politekhnicheskaya 29, 195251 St. Petersburg, Russia*
[4]*Helmholtz-Zentrum Dresden-Rossendorf, Institute of Ion Beam Physics and Materials Research, 01328 Dresden, Germany*
[5]*Experimentelle Physik 2, Technische Universität Dortmund, D-44221 Dortmund, Germany*
[6]*Experimentelle Physik 3, Technische Universität Dortmund, D-44221 Dortmund, Germany*

(Received 21 April 2018; accepted 20 July 2018; published online 7 August 2018)

All-optical thermometry technique based on the energy level cross-relaxation in atomic-scale spin centers in SiC is demonstrated. This technique exploits a giant thermal shift of the zero-field splitting for centers in the triplet ground state, S=1, undetected by photoluminescence (so called “dark” centers) coupling to neighbouring spin-3/2 centers which can be optically polarized and read out (“bright” centers), and does not require radiofrequency fields. EPR was used to identify defects. The width of the cross-relaxation line is almost an order of magnitude smaller than the width of the excited state level-anticrossing line, which was used in all-optical thermometry and which can not be significantly reduced since determined by the lifetime of the excited state. With approximately the same temperature shift and the same signal intensities as for excited state level-anticrossing, cross-relaxation signal makes it possible to increase the sensitivity of the temperature measurement by more than an order of magnitude. Temperature sensitivity is estimated to be approximately 10 mK/Hz$^{1/2}$ within a volume about 1 μ^3, allocated by focused laser excitation in a scanning confocal microscope. Using cross-relaxation in the ground states of “bright” spin-3/2 centers and “dark” S=1 centers for temperature sensing and ground state level anti-crossing of “bright” spin-3/2 centers an integrated magnetic field and temperature sensor with submicron space resolution can be implemented using the same spin system. The coupling of individually addressable “bright” spin-3/2 centers connected by a chain of “dark” S=1 spins, could be considered in quantum information processing and multicenter entanglement under ambient conditions.
https://doi.org/10.1063/1.5037158

Temperature sensing with high spatial resolution is required for monitoring of heat dissipation in electronic circuits, mapping of processes inside biochemical systems and other applications.[1–3] Using quantum-mechanical properties of the nitrogen-vacancy (NV) color centers in diamond, the temperature sensitivity of ~10mK/Hz$^{1/2}$ is achievable,[1–3] which is based on the thermal shift of the optically detected magnetic resonance (ODMR) frequency in the NV center[4] and the use of the advanced readout protocols, particularly thermal spin echo[1,3] or temperature-scanned ODMR.[5]

[a]E-mail: aan0100@gmail.com

Atomic-scale vacancy-related color centers in silicon carbide (SiC) have recently been proposed to form the basis for quantum spintronics, sensorics, and quantum information processing because of the unique properties of their electron spins, which can be optically polarized and read out by means of ODMR technique, energy level anticrossing (LAC) and cross-relaxation (CR).[6–22] A family of color centers with S = 3/2 ground and excited states (spin-3/2 centers), was shown to have the property of optical alignment of the spin levels and allow a spin manipulation. The experimental achievements in an all-optical thermometry technique is based on the excited state LAC (ES LAC) of spin-3/2 centers which exploits a giant thermal shift of the excited-state zero-field splitting (ZFS), and do not require RF fields.[12,14,17–21] A temperature sensitivity of ∼100mK/Hz$^{1/2}$ within a detection volume of approximately 10^{-6} mm^3 could be achieved.[17] An important advantage of using spin centers in SiC is optical compatibility with the band of transparency of fiber optics and biological objects, which minimizes the temperature effects on the object of investigation.

Giant temperature shift of CR signals has been detected in 15R-SiC single crystals. The width of the CR line is almost an order of magnitude smaller than the width of the ES LAC line that makes it possible to increase the temperature measurement sensitivity by approximately an order of magnitude.

15R-SiC single crystals with low concentration of nitrogen (∼10^{16} cm^{-3}) were grown by the Physical Vapor Transport method. The spin-3/2 centers were introduced by irradiation of the crystal with 1.4 MeV electrons, the fluence of ∼10^{18} cm^{-2}. The excitation into the vibronic sidebands of the spin centers in SiC was performed with wavelengths of 785 or 805 nm lasers with power in the range of several hundreds mW, and the PL is recorded in the spectral range from 850 to 1000 nm, allowing optical readout of the spin state. Lock-in detection of the PL variation for spin-3/2 centers was performed under application of constant (dc) and oscillating magnetic field with a typical frequency of 100–500 Hz, an amplitude ≤0.1 mT. To decrease the detection volume to approximately 10^{-9} mm^3 (1 μ^3) a scanning confocal microscope with near-infrared optimized objective of the company NT-MDT Spectrum Instruments was used. For the concentration of spin centers of about 10^{16} -10^{17} cm^{-3}, which was used in our experiments, in a volume of ∼1 μ^3 there are approximately 10^4-10^5 centers.

Figure 1 shows a general view of the PL variation ΔPL as a function of the dc magnetic field B with application of an additional oscillating magnetic field recorded at different temperatures in 15R-SiC single crystal, RF is not applied. PL was excited by a laser with a wavelength of 805 nm in a volume of ∼1 μ^3, allocated with a scanning confocal microscope. The lines indicate areas of magnetic fields where ground state LAC (GS LAC), ES LAC and CR signals for V2, V3 and V4 spin-3/2 centers are observed. The designations of the centers are tied to the energy of the zero-phonon lines: V2 - 886.5 nm, V3 - 904 nm, V4 - 917 nm.[18] The temperature varied in steps of approximately 3 degrees from 129 K to 257 K. For a temperature of 244 K, the signal ΔPL in the entire range of magnetic fields is given. The positions of the GS LACs are practically independent of temperature, while strong temperature shifts are visible for a wide line of the ES LAC and for a number of narrow CR lines.

Figure 2 shows EPR spectra (W-band, electron spin echo - ESE) observed in e-irradiated 15R-SiC crystal measured at orientation B || c at 100 K in darkness and under optical illumination with wavelength 789 nm.[19] Under the influence of light, an inverse phase is observed for the spin-3/2 centers (we will call them "bright" centers), whereas for S=1 centers with a large splitting between the lines, only a decrease in the distance between the lines is observed, due to the insignificant heating of the crystal ("dark" centers).

The standard spin Hamiltonian is given by

$$H = \gamma \mathbf{B.S} + \mathrm{D}[\mathbf{S_Z}^2 - 1/3\mathrm{S}(\mathrm{S}+1)]. \tag{1}$$

Systems with spin S=3/2 and S=1 and the same gyromagnetic ratio γ are considered, D is the axial fine structure splitting parameter. ZFS for the spin-3/2 centers Δ=2D, D(V2) = 69.5 MHz (2.48 mT), D(V3) = -5.6 MHz (-0.2 mT_, D(V4) = 25.2 MHz (0.9 mT).[18,21] One optically pumps V2 center into the M_S = ±3/2 states; V3 and V4 into the M_S = ±1/2 states.

The CR signals appear when the magnetic field tunes the spin splitting of "bright" spin-3/2 centers into resonance with the spin splitting of surrounding "dark" S=1 centers (inset in Fig. 2). Following

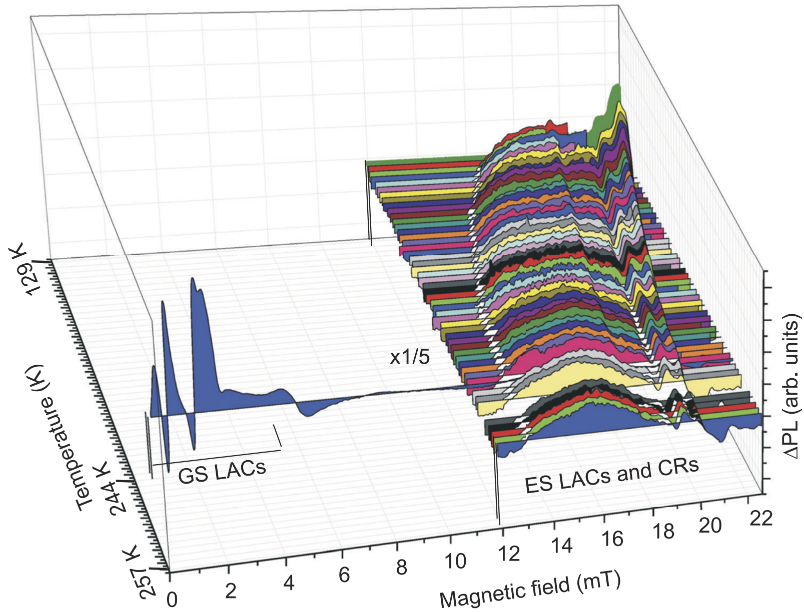

FIG. 1. Lock-in detection of the PL variation ΔPL as a function of the dc magnetic field B, recorded at different temperatures in 15R-SiC single crystal. ΔPL is caused by the application of an additional weak oscillating magnetic field, i.e., ΔBcosωt with ΔB = 100 μT and ω/2π = 0.5 kHz. The lines indicate areas of magnetic fields where GS LAC (for V2, V3 and V4 spin centers), ES LAC and CR signals are observed. RF is not applied. Photoluminescence was excited by a laser with a wavelength of 805 nm in a volume of ~1 μ^3, isolated with a confocal microscope. The temperature varied in steps of approximately 3 degrees from 129 K to 257 K. For a temperature of 244 K, the signal for changing the photoluminescence in the entire range of magnetic fields is given.

Ref. 23, where NV defects and N donors in diamond were considered as "bright" and "dark" centers, respectively, the dark-spin spectroscopy technique is applicable to a variety of paramagnetic defects in SiC. It is possible to register small numbers of "dark" centers neighbouring to single "bright" spin-3/2 center by monitoring of PL of single spin under ambient conditions. For example, the coupling of two individually addressable "bright" spin-3/2 centers connected by a chain of "dark" S=1 spins, could be considered in quantum information processing and multicenter entanglement.

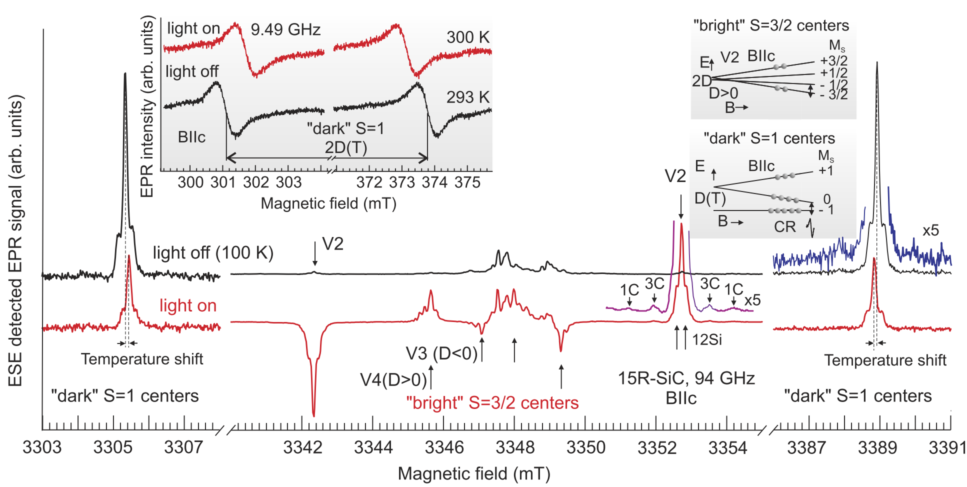

FIG. 2. ESE-detected EPR spectra (W-band) of "bright" S=3/2 and "dark" S=1 centers in e-irradiated 15R-SiC crystal at 100 K in darkness and under 789 nm optical illumination. Left inset: the EPR lines of the S = 1 center (X-band) near room temperature. Right inset: the energy level schemes for "bright" S=3/2 (V2) and "dark" S=1 centers and CR signal.

For “dark” S=1 center, D is strongly temperature dependent, this center seems was observed in Ref. 24. The inset shows the EPR lines of the “dark” S=1 center, recorded in the X-band near room temperature. The assignment of S=1 to the centers with D(T) was supported by our measuring the pulse length needed for the optimum signals in the ESE experiments. The “dark” centers have a certain analogy with the Si-C divacancies, since the parameter D(T) is close to the corresponding value for the divacancy,[6,25] and also the observed hyperfine (HF) structure (Fig. 2) with the nearest atoms of Si and C has common features. For divacancies HF interactions with 12 Si in the second coordination sphere break up into three groups of interactions (6, 3, 3), which leads to a broadening of the satellite lines and a decrease in their relative intensity; for “dark” centers this HF interaction is ~12 MHz. The interaction with three nearest neighboring carbons in basal plane is ~59 MHz and these HF interactions in a rough approximation correspond to the interaction observed for divacancies,[25] thus it can be assumed that the core of the “dark” S=1 center corresponds to a divacancy directed along the c-axis. Since there was no noticeable D temperature dependence for divacancies, we can assume the presence of a defect adjacent to the divacancy along the c-axis for the “dark” center, the position of which essentially depends on the temperature.

We equate the energy differences for the transitions between spin levels for “bright” S=3/2 centers, (the transitions that induce changes in the PL) and “dark” S=1 centers, as a result, we obtain B_{CR} at which CR occurs: $B_{CR}=|D(T)-2D|/2\gamma$.

Figure 3 shows evolution of the PL as a function of the dc magnetic field B, recorded at different temperatures in 15R-SiC single crystal. A circles with a dot at 0.2, 0.9 and 2.48 mT indicate the characteristic magnetic fields of different “forbidden” GS LAC labeled as GS LAC1 for V3, V4 and V2 centers, respectively (following to Refs. 20 and 21 we will call the LAC between the two levels with $\Delta M_S = \pm 1$ as “allowed” and with $\Delta M_S = \pm 2$ as “forbidden”). Vertical solid and dash lines reflect the absence of temperature dependence for D parameters for the GS LAC; solid lines are drawn for GS LAC1 ($B=D/\gamma$), dashed for “allowed” LACs denoted by LAC2 ($B=2D/\gamma$).

The oblique dashed lines reflect the changes in the position of the ES LAC points (squares, wide lines) and “bright-dark” CR (circles, narrow lines). The upper insert shows a shift in the CR lines with a temperature change from 161 K to 257 K. The lower insert shows a shift of one of the CR lines with a temperature change from 35 C to 42 C - possible temperature changes for the living system, a noise track is also shown.

The dotted line shows the the experimental points (crosses) from EPR measurements and simulated temperature dependence of the D(T)/2 for “dark” S=1 centers. In the range 180-300 K, the CR magnetic field B_{CR} versus temperature is reasonable to approximate by a linear function $B_{CR}= B_0 - k*T$; $\Delta B_{CR} = - k*\Delta T$. ΔB_{CR} can be then converted to temperature using $\Delta T = -\Delta B_{CR}/k$. For the most intense peaks CR1: $B_0 = 21.8$ mT; $k = 0.017$ mT/K; and CR2: $B_0 = 23.8$ mT; $k = 0.018$ mT/K.

The temperature field will be measured at different points when the SiC crystal plate is scanned in a microscope. In this case, the object under investigation, for example, in the form of a film, is placed directly on a plate of active material in the form of silicon carbide for thermal contact, the thermal conductivity of silicon carbide is very high and it is possible to study various thermal processes in the object of research (microelectronics chips, biological systems, where reactions take place with the release of heat, etc.). Additional advantage over the diamond is the lack of an RF field.

The level anticrossing in the ground state does not depend on temperature, this is an additional advantage, since one effects can be used to determine the magnetic field (GS LAC), and others – (CRs) to determine the temperature. In this case, the same spin system is used, the desired object is selected only by applying a bias in the form of a constant magnetic field.

The technique for measuring temperature can be expanded by using SiC nanocrystals with the spin centers. The advantage of using vacancy-related spin centers in SiC in comparison with NV centers diamond is the orientation of all spin centers along one axis, so instead of using single centers, it is convenient to use ensembles of such centers, which significantly increases the sensitivity of measurements. For example, a SiC nanocrystal with the spin centers can be placed on a probe of an atomic force microscope or a near field microscope that directly contact the object under study. Such measurements are carried out by us and will be published later.”

The noise limit of measurements with one scan without accumulation and the measurement time of about 0.1 sec is 3 μT (in the slope of the derivative). The seven degrees of the thermometer

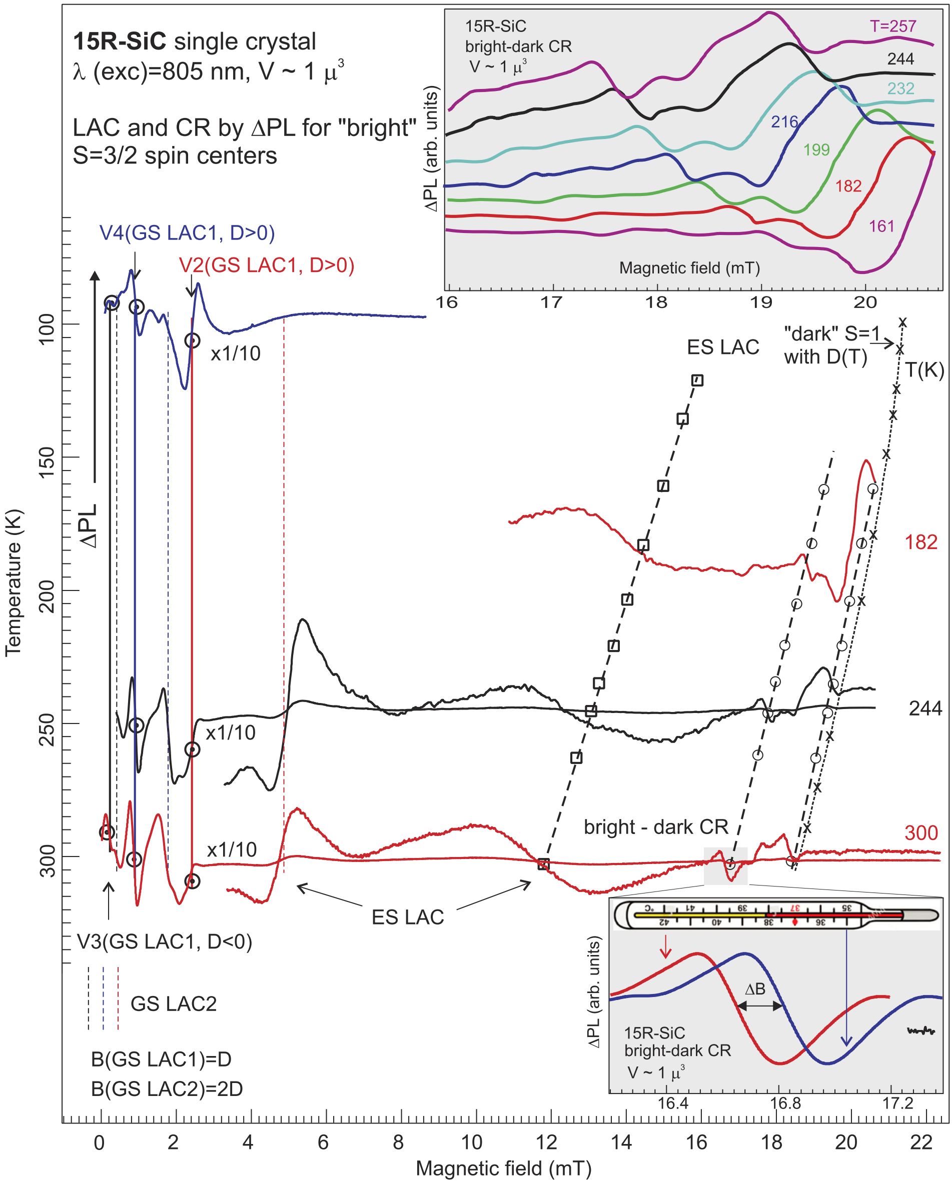

FIG. 3. Lock-in detection of the PL variation ΔPL as a function of the dc magnetic field B, recorded at different temperatures in 15R-SiC single crystal. ΔPL is caused by the application of an additional weak oscillating magnetic field. RF is not applied. A circle with a dot indicates the characteristic magnetic fields of different "forbidden" LACs denoted by LAC1 (B=D) for the ground state of the spin-3/2 center. Vertical solid and dashed lines reflect the absence of a change in the parameters of the fine structure (D) for the ground state of the spin centers with a change in temperature; solid lines are drawn for LAC1, dashed for "allowed" LACs denoted by LAC2 (B=2D). The oblique dashed lines reflect the changes in the position of the LAC points for the excited state of the spin-3/2 centers (squares, wide lines) and cross-relaxation (circles, narrow lines). The upper insert shows a shift in the "bright-dark" cross-relaxation lines with a temperature change from 161 K to 257 K. For greater clarity, in the upper inset, the temperature increases in the opposite direction as compared to the main part of the figure. The lower insert shows a shift of one of the cross-relaxation lines with a temperature change from 35 C to 42 C - possible temperature changes for the living system. A noise track is shown. The dotted line shows the simulated temperature dependence of the fine structure splitting (as D/2) for "dark" spin-1 centers, the crosses denote the experimental points from EPR measurements.

(42 C-35 C) corresponds to a shift of ~180 mkT (Fig. 3, bottom inset), that is 180 mkT/7 K = 25 mkT/K. It can be estimated that the sensitivity is approximately 100 mkK/Hz$^{1/2}$. At lower temperatures, we have sensitivity about five times higher, since the signal intensity has increased approximately 5 times (Fig. 3, upper inset), that is, less than 20 mK/Hz$^{1/2}$. When selecting more sensitive detectors and optimizing the optical circuit, it is possible to achieve less then 10 mK/Hz$^{1/2}$ in the volum of 1 μ^3.

For the concentration of spin centers of about 10^{16} -10^{17} cm^{-3}, which was used in our experiments, in a volume of ~1 μ^3 there are approximately 10^4-10^5 centers.

This work was supported by the by the RFBR under Grant No. 16-02-00877-a; by the Russian Academy of Sciences; and the DFG in the frame of ICRC TRR 160. V.A.S. acknowledges support through a sponsorship provided by the Alexander von Humboldt (AvH) foundation fellowship.

[1] P. Neumann, I. Jakobi, F. Dolde, C. Burk, R. Reuter, G. Waldherr, J. Honert, T. Wolf, A. Brunner, J. H. Shim, D. Suter, H. Sumiya, J. Isoya, and J. Wrachtrup, Nano Letters **13**, 2738 (2013).
[2] G. Kucsko, P. C. Maurer, N. Y. Yao, M. Kubo, H. J. Noh, P. K. Lo, H. Park, and M. D. Lukin, Nature **500**, 54 (2013).
[3] D. M. Toyli, C. F. de las Casas, D. J. Christle, V. V. Dobrovitski, and D. D. Awschalom, Proc. Natl. Acad. Sci. **110**, 8417 (2013).
[4] V. M. Acosta, E. Bauch, M. P. Ledbetter, A. Waxman, L.-S. Bouchard, and D. Budker, Phys. Rev. Lett. **104**, 070801 (2010).
[5] R. A. Babunts, A. A. Soltamova, D. O. Tolmachev, V. A. Soltamov, A. S. Gurin, A. N. Anisimov, V. L. Preobrazhenskii, and P. G. Baranov, JETP Letters **95**, 429 (2012).
[6] P. G. Baranov, I. V. Il'in, E. N. Mokhov, M. V. Muzafarova, S. B. Orlinskii, and J. Schmidt, JETP Lett. **82**, 441 (2005).
[7] P. G. Baranov, A. P. Bundakova, I. V. Borovykh, S. B. Orlinskii, R. Zondervan, and J. Schmidt, JETP Lett. **86**, 202 (2007).
[8] J. R. Weber, W. F. Koehl, J. B. Varley, A. Janotti, B. B. Buckley, C. G. Van de Walle, and D. D. Awschalom, Proc. Natl. Acad. Sci. **107**, 8513 (2010).
[9] D. DiVincenzo, Nat. Mater. **9**, 468 (2010).
[10] P. G. Baranov, A. P. Bundakova, A. A. Soltamova, S. B. Orlinskii, I. V. Borovykh, R. Zondervan, R. Verberk, and J. Schmidt, Phys. Rev. B **83**, 125203 (2011).
[11] D. Riedel, F. Fuchs, H. Kraus, S. Vath, A. Sperlich, V. Dyakonov, A. Soltamova, P. Baranov, V. Ilyin, and G. V. Astakhov, Phys. Rev. Lett. **109**, 226402 (2012).
[12] H. Kraus, V. A. Soltamov, F. Fuchs, D. Simin, A. Sperlich, P. G. Baranov, G. V. Astakhov, and V. Dyakonov, Scientific Reports **4**, 5303 (2014).
[13] S. G. Carter, Ö. O. Soykal, P. Dev, S. E. Economou, and E. R. Glaser, Physical Review B **92**, 161202 (2015).
[14] D. Simin, V. A. Soltamov, A. V. Poshakinskiy, A. N. Anisimov, R. A. Babunts, D. O. Tolmachev, E. N. Mokhov, M. Trupke, S. A. Tarasenko, A. Sperlich, P. G. Baranov, V. Dyakonov, and G. V. Astakhov, Phys. Rev. X **6**, 031014 (2016).
[15] M. Widmann, S.-Y. Lee, T. Rendler, N. T. Son, H. Fedder, S. Paik, L.-P. Yang, N. Zhao, S. Yang, I. Booker, A. Denisenko, M. Jamali, S. Ali Momenzadeh, I. Gerhardt, T. Ohshima, A. Gali, E. Janzén, and J. Wrachtrup, Nature Materials **14**, 164 (2015).
[16] D. J. Christle, A. L. Falk, P. Andrich, P. V. Klimov, J. u. Hassan, N. T. Son, E. Janzén, T. Ohshima, and D. D. Awschalom, Nature Materials **14**, 160 (2015).
[17] A. N. Anisimov, D. Simin, V. A. Soltamov, S. P. Lebedev, P. G. Baranov, G. V. Astakhov, and V. Dyakonov, Scientific Reports **6**, 33301 (2016).
[18] V. A. Soltamov, B. V. Yavkin, D. O. Tolmachev, R. A. Babunts, A. G. Badalyan, V. Yu. Davydov, E. N. Mokhov, I. I. Proskuryakov, S. B. Orlinskii, and P. G. Baranov, Phys. Rev. Lett. **115**, 247602 (2015).
[19] G. V. Astakhov, D. Simin, V. Dyakonov, B. V. Yavkin, S. B. Orlinskii, I. I. Proskuryakov, A. N. Anisimov, V. A. Soltamov, and P. G. Baranov, Appl. Magn. Reson. **47**, 793 (2016).
[20] A. N. Anisimov, V. A. Soltamov, E. N. Mokhov, P. G. Baranov, G. V. Astakhov, and V. Dyakonov, Appl. Magn. Reson. **49**, 85 (2018).
[21] P. G. Baranov, H.-J. von Bardeleben, F. Jelezko, and J. Wrachtrup, Magnetic Resonance of Semiconductors and Their Nanostructures: Basic and Advanced Applications: Springer Series in Materials Science Volume 253 (2017).
[22] H. J. von Bardeleben, J. L. Cantin, E. Rauls, and U. Gerstmann, Phys. Rev. B **92**, 064104 (2015).
[23] R. I. Epstein, F. M. Mendoza, Y. K. Kato, and D. D. Awschalom, Nature Physics **1**, 94 (2005).
[24] N. M. Pavlov, M. I. Iglitsyn, M. G. Kosaganova, and V. N. Solomatin, Sov. Phys. Semicond. **9**, 845 (1975).
[25] N. T. Son, P. Carlsson, J. ul Hassan, E. Janzen, T. Umeda, J. Isoya, A. Gali, M. Bockstedte, N. Morishita, T. Ohshima, and H. Itoh, Phys. Rev. Lett. **96**, 055501 (2006).